

AD-A093 489

HERIOT-WATT UNIV EDINBURGH (SCOTLAND) DEPT OF PHYSICS F/6 20/5,
SUBMILLIMETER LASER AND FABRY-PEROT SPECTROSCOPY USING METALLIC--ETC(U)
MAY 79 C R PIDGEON, B W DAVIS DA-ERO-78-6-074

UNCLASSIFIED

NL

1
2
3
4
5
6
7
8
9
10
11
12

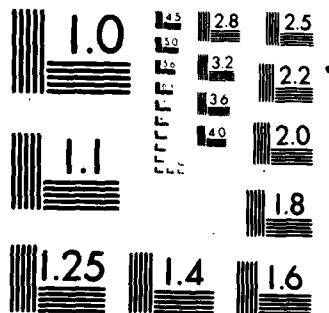
END

DATE

FILED

2 81

DTIC



MICROCOPY RESOLUTION TEST CHART
NATIONAL BUREAU OF STANDARDS 1963 A

UNCLASSIFIED

SECURITY CLASSIFICATION OF THIS PAGE (When Data Entered)

R&D 2543-EE

REPORT DOCUMENTATION PAGE		READ INSTRUCTIONS BEFORE COMPLETING FORM	
1. REPORT NUMBER		2. GOVT ACCESSION NO.	
		AD-A093 489	
3. TITLE (and Subtitle)		4. RECIPIENT'S CATALOG NUMBER	
Submillimeter Laser and Fabry-Perot Spectroscopy Using Metallic Mesh.		9	
5. AUTHOR(s)		6. TYPE OF REPORT & PERIOD COVERED	
Dr. C.R. Pidgeon Mr. B.W. Davis		1st Annual Technical Report 1 Jun 78 - 31 May 79	
7. PERFORMING ORGANIZATION NAME AND ADDRESS		8. PERFORMING ORG. REPORT NUMBER	
Heriot-Watt University Riccarton, Edinburgh, U.K.			
9. CONTRACT OR GRANT NUMBER(s)		10. PROGRAM ELEMENT, PROJECT, TASK AREA & WORK UNIT NUMBERS	
DA-ERD-78-G-074		6.11.02a 1T161102BH57-03 17 03	
11. CONTROLLING OFFICE NAME AND ADDRESS		12. REPORT DATE	
USARDSG-UK Box 65, FPO NY 09510		May 79	
13. MONITORING AGENCY NAME & ADDRESS (if different from Controlling Office)		14. NUMBER OF PAGES	
		18 12 20	
		15. SECURITY CLASS. (of this Report)	
		Unclassified	
		15a. DECLASSIFICATION/DOWNGRADING SCHEDULE	
16. DISTRIBUTION STATEMENT (of this Report)			
Approved for Public Release; Distribution Unlimited			
17. DISTRIBUTION STATEMENT (of the abstract entered in Block 20, if different from Report)			
18. SUPPLEMENTARY NOTES			
19. KEY WORDS (Continue on reverse side if necessary and identify by block number)			
Fabry-Perot Spectroscopy; CO ₂ Laser; Submillimeter Laser Spectroscopy; Metallic Mesh Spectroscopy; Heterodyne Techniques			
20. ABSTRACT (Continue on reverse side if necessary and identify by block number)			
The performance of an optically pumped submillimeter laser is directly dependent on the infrared (CO ₂) pump used, and the importance of the pump laser in relation to the tuning and stability characteristics has necessitated extensive investigations being carried out on the pump laser. This CO ₂ laser would later be used in conjunction with the submillimeter laser at present being completed.			

DD FORM 1473
1 JAN 73

EDITION OF 1 NOV 65 IS OBSOLETE

UNCLASSIFIED

SECURITY CLASSIFICATION OF THIS PAGE (When Data Entered)

UNCLASSIFIED

SECURITY CLASSIFICATION OF THIS PAGE(When Data Entered)

20. Cont.

Heterodyning techniques using an optogalvanically stabilized CO₂ laser as a reference were used to determine the mode profile and tuning characteristics of the main CO₂ pump laser. In addition to heterodyne measurements, mode profiles were also observed at the laser output and at 3m distant using short exposures of heat sensitive paper. After optimization of the laser a tuning range of ~ 35 MHz about the natural CO₂ line centre on the TEM₀₀ mode was obtained. The short term stability of the CO₂ laser has been measured as less than ± 0.7 MHz, this being limited by the jitter modulation of the reference laser.

Transmission measurements have been made on metallic mesh which would be used in conjunction with the submillimeter laser under construction. The samples investigated were of the inductive and capacitive type and are commercially available.

UNCLASSIFIED

SECURITY CLASSIFICATION OF THIS PAGE(When Data Entered)

Summary

The performance of an optically pumped submillimetre laser is directly dependent on the infrared (CO₂) pump used, and the importance of the pump laser in relation to the tuning and stability characteristics has necessitated extensive investigations being carried out on the pump laser. This CO₂ laser would later be used in conjunction with the submillimetre laser at present being completed.

Heterodyning techniques using an optogalvanically stabilized CO₂ laser as a reference were used to determine the mode profile and tuning characteristics of the main CO₂ pump laser. In addition to heterodyne measurements, mode profiles were also observed at the laser output and at 3m distant using short exposures of heat sensitive paper. After optimization of the laser a tuning range of ~ 35 MHz about the natural CO₂ line centre on the TEM₀₀ mode was obtained. The short term stability of the CO₂ laser has been measured as less than ± 0.7 MHz, this being limited by the jitter modulation of the reference laser.

Transmission measurements have been made on metallic mesh which would be used in conjunction with the submillimetre laser under construction. The samples investigated were of the inductive and capacitive type and are commercially available.

Keywords: CO₂ laser; submillimetre laser; heterodyne techniques; metallic mesh.

Accession For	
NTIS GFA&I	<input checked="checked" type="checkbox"/>
DTIC TAB	<input type="checkbox"/>
Unannounced	<input type="checkbox"/>
Justification	
By	
Distribution/	
Availability Codes	
Dist	Avail and/or Special
A	

Table of Contents

	Page
Chapter 1 A Pump Laser for a Submillimetre Laser	5
1.1 Introduction	5
1.2 The CO ₂ Laser	5
1.3 Heterodyne Techniques used to determine Characteristics of the CO ₂ Pump Laser	6
1.3.1 Mode Structure and Tuning Characteristics of the CO ₂ Laser	7
1.3.2 Stability Measurements	8
1.4 Cooling Effects	8
Chapter 2 Transmission Characteristics of Metallic Mesh	9
2.1 Introduction	9
2.2 The Inductive Mesh	11
2.3 The Capacitive Mesh	11

List of Figures and Tables

Chapter 2

- Figure 2.1 Transmission profiles of inductive meshes,
100 L.P.I. to 500 L.P.I.
- Figure 2.2 Transmission profiles of inductive meshes,
750 L.P.I. to 1500 L.P.I.
- Figure 2.3 Comparison of 1000 L.P.I. inductive meshes
with different ϵ_0 values.
- Figure 2.4 Typical capacitive mesh profile ('g' value
= 100 μm .)

Tables

- 2.1 Details of available inductive meshes.
- 2.2 Details of available capacitive meshes.

Chapter 1

A Pump Laser for a Submillimetre Laser

1.1 Introduction

The cw CO₂ laser intended for use as a pump laser in the testing of the submillimetre laser under construction has been extensively investigated. A description of the laser will be given followed by the method by which the characteristics of the same laser were obtained.

Although the absorption lines of vibrational-rotational molecular transitions commonly used as driving transitions in optically pumped submillimetre lasers are typically Doppler broadened to ~ 50 MHz full width half maximum (F.W.H.M.), the operating pressures of cw lasers are normally restricted to pressures well below 1 torr, where pressure broadening is only ~ 1 MHz. The narrow radiation linewidth produced by a cw CO₂ laser therefore selectively excites only a small fraction of the available molecules, those with Doppler-shifted absorption frequencies lying within the homogeneous linewidth of the actual CO₂ laser frequency. Tuning of the CO₂ laser, by means of a piezo-ceramic attached to the output coupler, over its pressure broadened gain linewidth of ~ 3.5 MHz/torr will therefore selectively excite different groups of molecules lying under the Doppler envelope, resulting in a corresponding tuning of the peak of the submillimetre gain. Since the finesse of typical submillimetre resonators is high, changes in the CO₂ laser frequency due to thermal shifts, mechanical instabilities or mode changes are accordingly strongly reflected in the submillimetre output power level. The consequence of this is that the CO₂ laser should have well controlled and stable frequency tuning characteristics if a stable submillimetre laser output is to be achieved.

1.2 The CO₂ Laser

The cw CO₂ laser investigated is of conventional design, comprising of a sealed water cooled 10 mm ID discharge tube with an internal 10 m concave semitransparent (30%) output coupler and an adjustable blazed diffraction grating. The 1.78 m optical resonator is supported by a strong structure of granite and four 1" thick invar bars, giving good mechanical and thermal stability. The laser could be operated in a 'sealed' or 'flowing' gas mode, but all of the results presented are for sealed operation. Flowing gas operation, although resulting in higher output powers, does have a detrimental effect on the frequency stability of the laser. The sealed off gas mix used is described:

15.3% $^{13}\text{C}^{16}\text{O}_2$, 14.2% N_2 , 4% Xe, 2% H, 64.4% He

cw output power levels of 15 W at band centre are easily available using the gas mix described.

Cooling of the gas mix has been found to improve power output and also increase the number of lasing lines, and this is discussed in section 1.4. The mix is an isotopic one with the normal ^{12}C being isotopically enriched to ^{13}C . This gas mix has been investigated with the view to using the new laser frequencies available from such a mix to generate new submillimetre laser frequencies. Such a sealed off isotopic mix can be used for ~ 1 -2 months with no sign of degradation in performance.

1.3 Heterodyne Techniques used to Determine Characteristics of the Pump CO_2 Laser

To determine the frequency stability and tuning characteristics of the CO_2 laser, a heterodyning technique was used. This is a relatively simple technique which uses two near coincident frequencies from different sources to give sum and difference beat frequencies, from which information about one of the sources can be derived. To enable measurements of any meaning to be made, however, one of the sources must be fixed in frequency. Any instabilities in the other source may then be observed, relative to the fixed laser source.

The method was to mix the laser outputs from the two CO_2 lasers one of which was optogalvanically stabilized*. The optogalvanically stabilized laser was of similar design to the main laser, but with a 1 metre cavity and with passive stability provided by three 1" diameter invar bars. Active stabilization was provided by the method now described.

An electronic feedback loop system was used to control the laser cavity length. The cavity length was modulated through the piezoceramic which was attached to the output coupler. The effect of the cavity length modulation is to give a modulation of the internal field intensity*, and any changes in this intensity are seen in the discharge impedance which can then be seen as a current fluctuation (the optogalvanic effect). A d.c. correction voltage is then applied to the piezoceramic to maintain oscillation at line centre. By this method the reference laser could be locked to $\sim \pm 0.2$ MHz of the natural line centre of the lasing transition.

* A L S Smith, S Moffat, Opt. Commun., Vol. 30 No. 2, Aug. 1979, p. 213.

For frequency measurements, a small fraction of the main CO_2 beam is split off with a NaCl beam splitter and mixed with the beam from the optogalvanically locked CO_2 reference laser.

The mixed outputs were then incident onto a PbSnTe liquid nitrogen cooled detector and the resultant beat note generated then displayed on a spectrum analyzer, immediately indicating the frequency components present in the main CO_2 laser beam. By observation of the displayed signal it was possible to determine the stability and tuning range of the CO_2 laser.

1.3.1 Mode Structure and Tuning Characteristics of the CO_2 Laser

In describing the results of the measurements made, it is convenient to distinguish between CO_2 laser lines at the band centres and on the band wings. The lines lying close to the band wings, where the laser gain is lower, were observed to always produce a single beat note on the spectrum analyzer, tunable piezoelectrically by up to ~ 35 MHz about the natural CO_2 line centre. The corresponding far field mode pattern was always circularly symmetric and uniform, indicating that the mode observed was the TEM_{00} mode. Burn patterns, on heat sensitive paper, close to the laser output were generally complex, and not of a Gaussian appearance; this is attributed to rapidly divergent rays of the same frequency as the TEM_{00} mode, perhaps caused by internal scattering or wall reflections within the discharge tube.

Laser lines lying near the centre of the CO_2 bands were generally found to contain three distinct frequency components: a single frequency, together with two other closely spaced frequencies (about 0.5 MHz apart) lying about 17 MHz higher in frequency. All frequencies tuned at the same rate as the piezoelectric drive were varied, maintaining their relative separations. It was found to be a simple practical matter to reduce the laser discharge current steadily until either the "single" frequency or the "double" frequency ceased to oscillate, so that essentially single frequency oscillation was obtained (i.e. that of the component lying closest to the gain centre). In this manner it was possible to operate the laser with the "single" frequency oscillating alone at frequencies lower than the natural CO_2 line centre, and with the "doublet" completely alone over all frequencies higher than the natural CO_2 line centre. Using these two regimes of operation, it was found that the single frequency was characterised by a Gaussian-like far field burn pattern, whilst the "doublet" was characterised by a more complex pattern (commonly an annulus) critically dependent upon fine adjustment of the diffraction grating.

Inspection of the standard expression for the mode frequencies of an open resonator shows that the Gaussian TEM_{00} mode should always be the lowest frequency present, in agreement with the above

observation. The "doublet" mode lying 17 MHz higher in frequency is most probably the almost degenerate TEM_{01} and TEM_{10} modes.

1.3.2 Stability Measurements

The short term instability of the output frequency was better than 100 kHz over a 1 sec period and was less than the jitter modulation of the reference heterodyne laser (± 0.7 MHz). The rigid mechanical construction of the laser enabled moderate shocks near the laser to perturb the laser frequency by less than 1 MHz, and under normal laboratory room conditions the thermal stability of the structure was sufficient to produce thermal drifts of less than 1.6 MHz over a ten minute period.

The measurements presented have confirmed that the cw CO_2 laser will be suitable for optically pumping a submillimetre laser.

1.4 Cooling Effects

The effect of varying the temperature of the cooling supply used with the isotopic gas mix has been investigated. It has been shown that increased performance is achieved by cooling of the supply down to $\sim -60^\circ C^*$, but in the work carried out the optimum was found to be at $0^\circ C$. The laser was cooled with a continuous flow of ethylene glycol at a temperature of $-15^\circ C$ and the output power from the laser monitored as the temperature was allowed to rise. The change in output power was ~ 0.1 W/ $^\circ C$, with the optimum found at $0^\circ C$. The power observed was 3.5 Watts at $0^\circ C$, but this power was later increased by suitable adjustments to pressure and discharge current. Another apparent advantage of cooling the isotope mix was seen in the increase in the number of laser lines present. At room temperature very few emission lines were observed (~ 9 total).

The relative ease of operation in sealed conditions, linked with the long lifetime of one fill of gas could make the isotopic CO_2 laser an extremely useful source of I.R. frequencies. The realization of the application of this type of laser in optical pumping will only be seen after work is carried out to investigate the possibilities of any frequency coincidences between the I.R. frequencies and the absorption lines in polar molecular species.

* C Freed, A H M Ross, R G O'Donnel, J. Mol. Spec., Vol. 49, p. 439, (1974).

Chapter 2

Transmission Characteristics of Metallic Mesh

2.1 Introduction

The use of metallic mesh in submillimetre work is necessary due to the excessive absorption experienced by other materials. Two types of metallic mesh are described within this report. The first is termed "inductive", and is a periodic array of holes in a thin metal foil of some finite thickness, and the second, "capacitive" is a periodic array of metal squares supported by some substrate. The description inductive and capacitive come from an analogy with transmission line equivalent circuits. The holes (or squares) are usually square and the subsequent $\pi/2$ symmetry eliminates any polarization effects.

A plane electromagnetic wave incident on such structures cause surface currents and charges to be set up in the metal and these act as secondary sources of electromagnetic radiation. In turn these secondary sources give rise to zero order transmitted and reflected waves of equal amplitude, and after scattering the original wave and the zero order transmitted wave superpose to give the total transmitted wave. Both types of mesh are characterised by two parameters which are: the mesh periodicity (g) and the spacing between the squares, $2a$.

If the zero order reflection coefficient has a complex amplitude $r(\omega)$, then we describe the transmitted wave amplitude by the fundamental relation,

$$t_I(\omega) = 1 + r_I(\omega) \quad (2.1)$$

If losses are neglected we can write equation (2.1) as

$$|t_I(\omega)|^2 + |r_I(\omega)|^2 = 1 \quad (2.2)$$

These expressions are for the inductive mesh, and the expressions for the capacitive mesh can be derived using the electromagnetic equivalent of Babinet's principle which relates the electromagnetic diffraction fields around a thin, perfectly conducting perforated screen with the fields around the complementary screen. Thus by applying Babinet's principle we have:

$$t_I(\omega) + t_C(\omega) = 1 \quad (2.3)$$

$$\text{giving } t_I(\omega) = r_C(\omega) \quad (2.4)$$

$$t_C(\omega) = -r_I(\omega)$$

where I and c refer to inductive and capacitive respectively.

Absorption has been neglected in the previous description but must be accounted for. Absorption results from ohmic losses of the surface currents flowing in the metallic sections of the grids and also from dielectric losses in the substrate supporting the capacitive mesh.

The absorption is given by,

$$A = |r(\omega)|^2 \left(\frac{c}{\lambda \sigma} \right)^{\frac{1}{2}} f \quad (2.5)$$

where $|r(\omega)|^2$ is the reflectivity, σ is the d.c. conductivity and f is a geometric factor, which is the amount of grid which can conduct current and is given by: for the inductive grid,

$$f_{IN} = g/2a,$$

and for the capacitive grid by,

$$f_{CAP} = \frac{1}{1-2a/g}$$

Looking at equation (2.5) it is evident that in order to reduce the effect of absorption losses, the conductivity should be as high as possible. The most obvious choice would be gold, but the cost is prohibitive. The commonly used metals are copper, nickel and aluminium.

The power transmission is described for a capacitive mesh by,

$$T = \frac{b^2 + z_0 (\omega/\omega_0 - \omega_0/\omega)^2}{(1+b)^2 + z_0^2 (\omega/\omega_0 - \omega_0/\omega)^2} \quad (2.6)$$

where $\omega = g/\lambda$, $\omega_0 = g/\lambda_0$, and $b = (c/\lambda\sigma)^{\frac{1}{2}}$. This expression is derived from the equivalent circuit description. The term $(\omega/\omega_0 - \omega_0/\omega)$ is the generalized frequency. ω_0 is the resonant normalized frequency and λ_0 is the frequency at which the capacitive mesh transmission is a minimum (a maximum for the inductive mesh).

For an idealized mesh with no losses, this factor, ω_0 would be unity.

z_0 is known as the characteristic impedance of the mesh and is given by

$$z_0^c = \frac{1}{\ln \operatorname{cosec}(\frac{\pi a}{2g})} \quad (2.7)$$

The complimentary relation, $z_0^c \cdot z_0^I = 1$ gives rise to the impedance relation for the inductive mesh.

It is evident that any desired level of reflectivity and transmissivity can be achieved by varying the g and a/g values. Transmission measurements for inductive and capacitive mesh of various g values have been made and are now discussed.

2.2 The Inductive Mesh

Electroformed inductive mesh was available in the range; 100 lines per inch to 1500 lines per inch. The individual pieces of mesh were stretched over a support ring and secured with flexible collodion, and the transmission profiles were subsequently measured with the aid of a Michelson FS720 Interferometer. Figures (2.1) and (2.2) show the coverage available with the meshes used and also display the characteristic profile of the inductive meshes. The range shown is 0 cm^{-1} to 500 cm^{-1} . The steepness of the slopes is governed by a/g value and this is seen in Fig. (2.2) and (2.3). From the data given for 750 l pi meshes in Fig. (2.2) and for the three 1000 l pi meshes presented in Fig. (2.3) it is seen that steeper transmissivity profiles result from larger a/g values.

Calculations using the complimentary relation to equation (2.7) give, in conjunction with the data derived from Figs. (2.1)-(2.3) the a/g values for each mesh.

The complimentary relation is given by

$$z_0^I = \ln \operatorname{cosec} (\pi a/2g) \quad (2.8)$$

The value, z_0^I was determined from the theoretical fit with the measured profile of the mesh under investigation. Substitution of this value gave the a/g values and these are given in table (2.1).

2.3 Capacitive Mesh

The capacitive mesh is produced by a photo-etching process with a metal thickness of around $\sim 0.2 \mu\text{m}$. Capacitive meshes could be produced by the evaporation of metal through an inductive mesh onto a substrate. Figure (2.4) shows a typical capacitive mesh profile,

indicating the complimentary nature of the two forms of mesh. Table (2.2) presents the necessary details on the capacitive mesh available.

Absorption losses for the metallic mesh have been found to be less than $\sim 1\%$, this being limited by the measuring process.

The data gathered on the metallic mesh described will later be used to design devices which will be used in conjunction with the soon to be completed submillimetre laser.

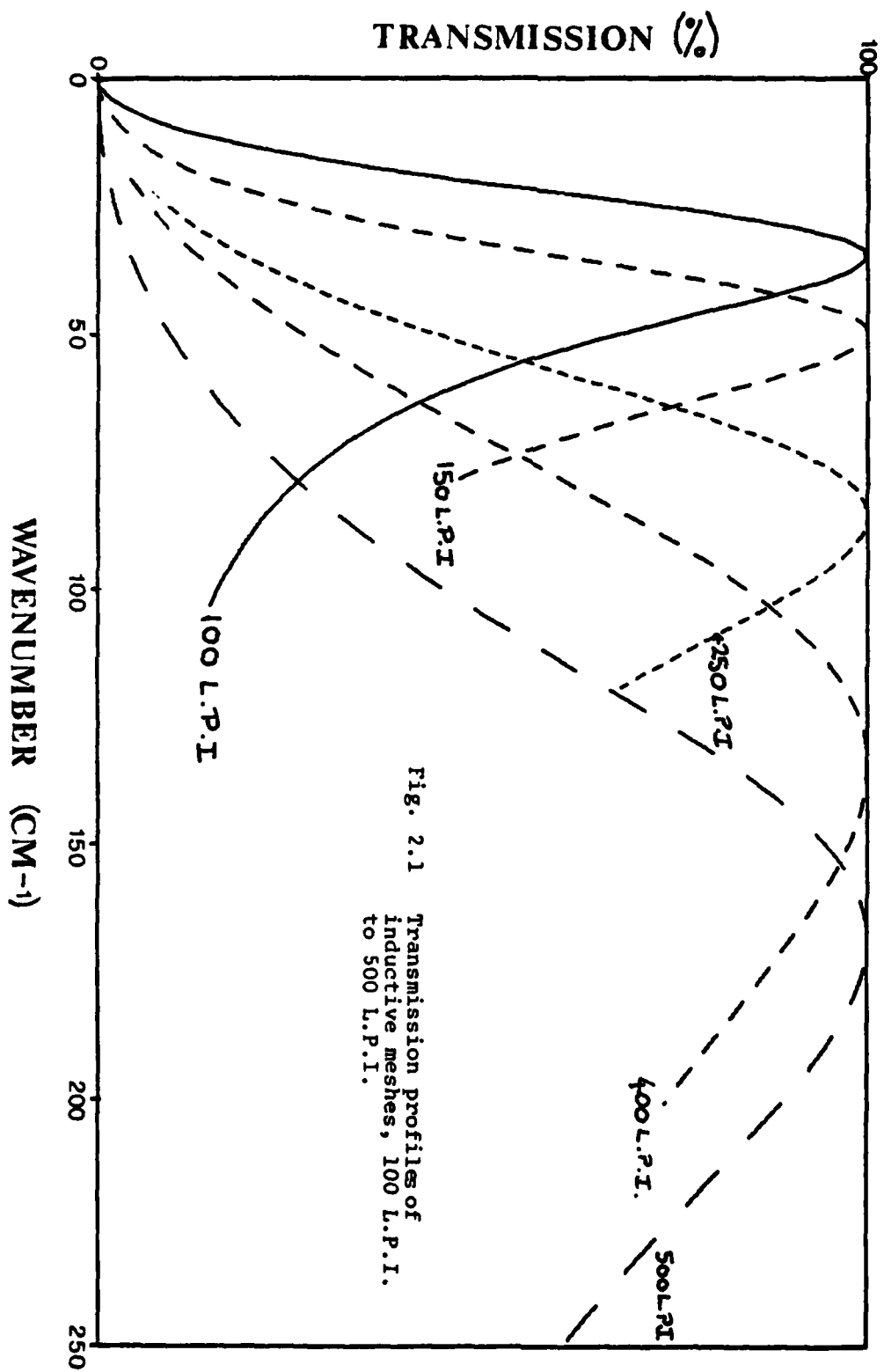
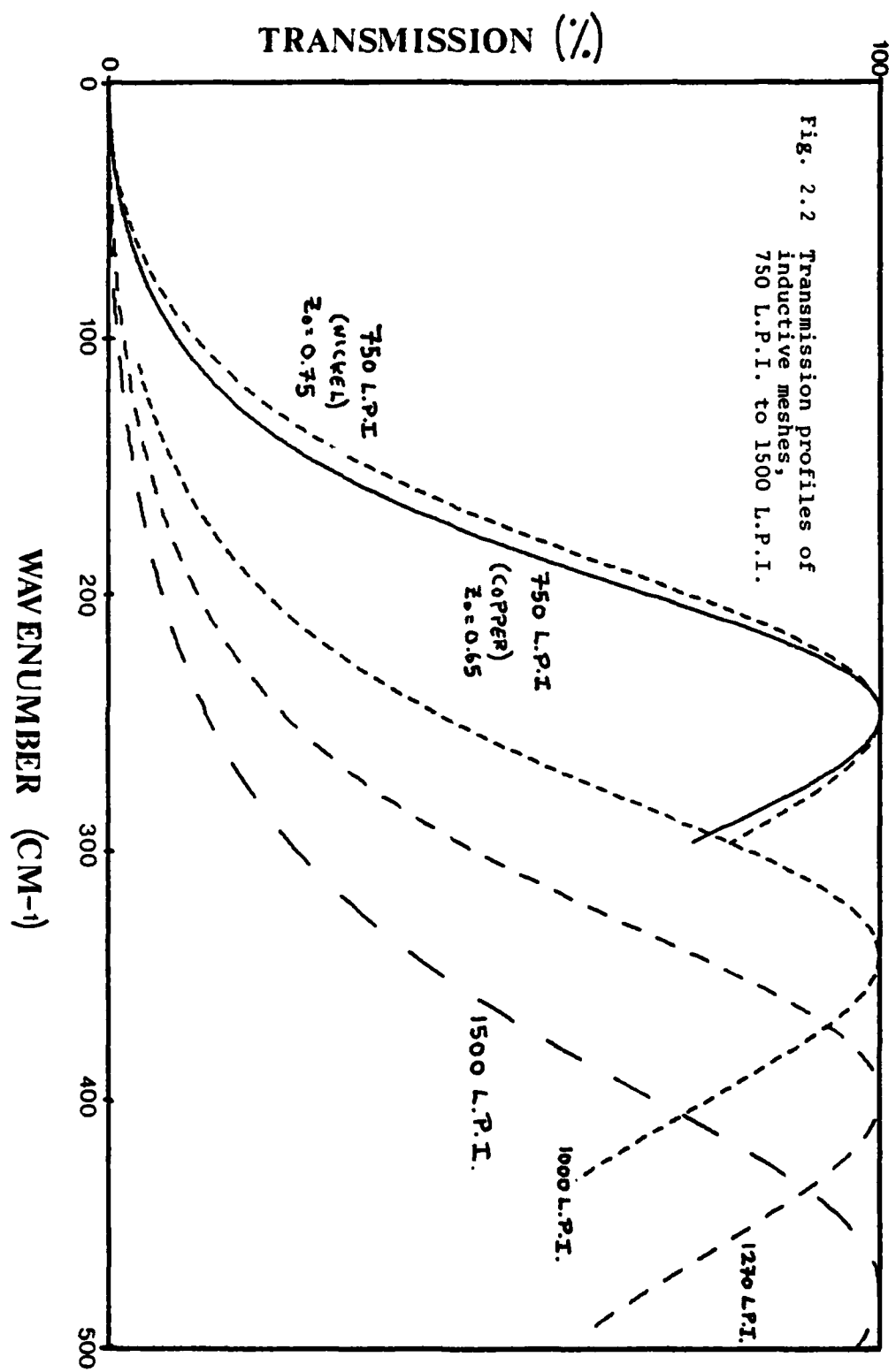
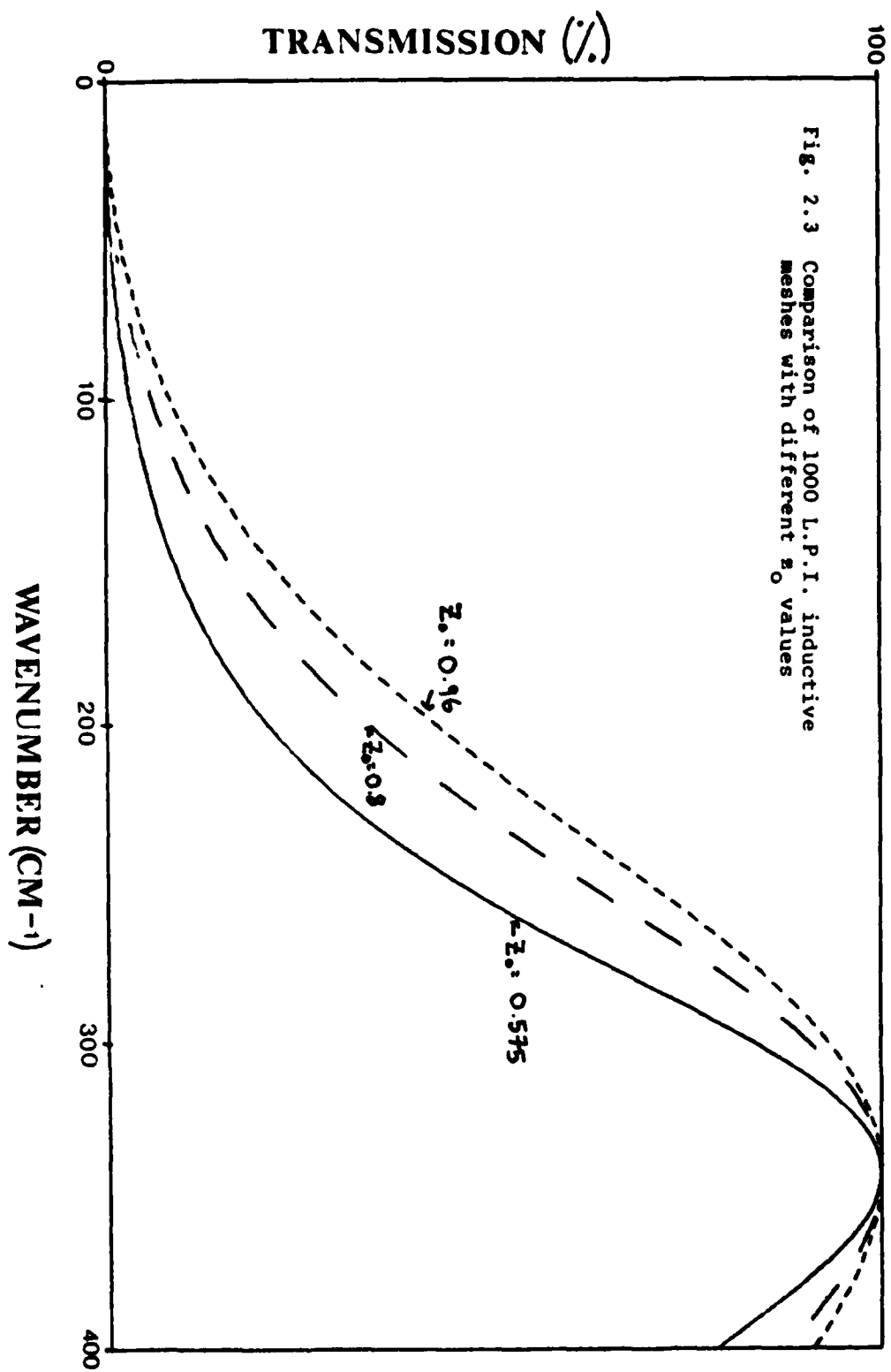
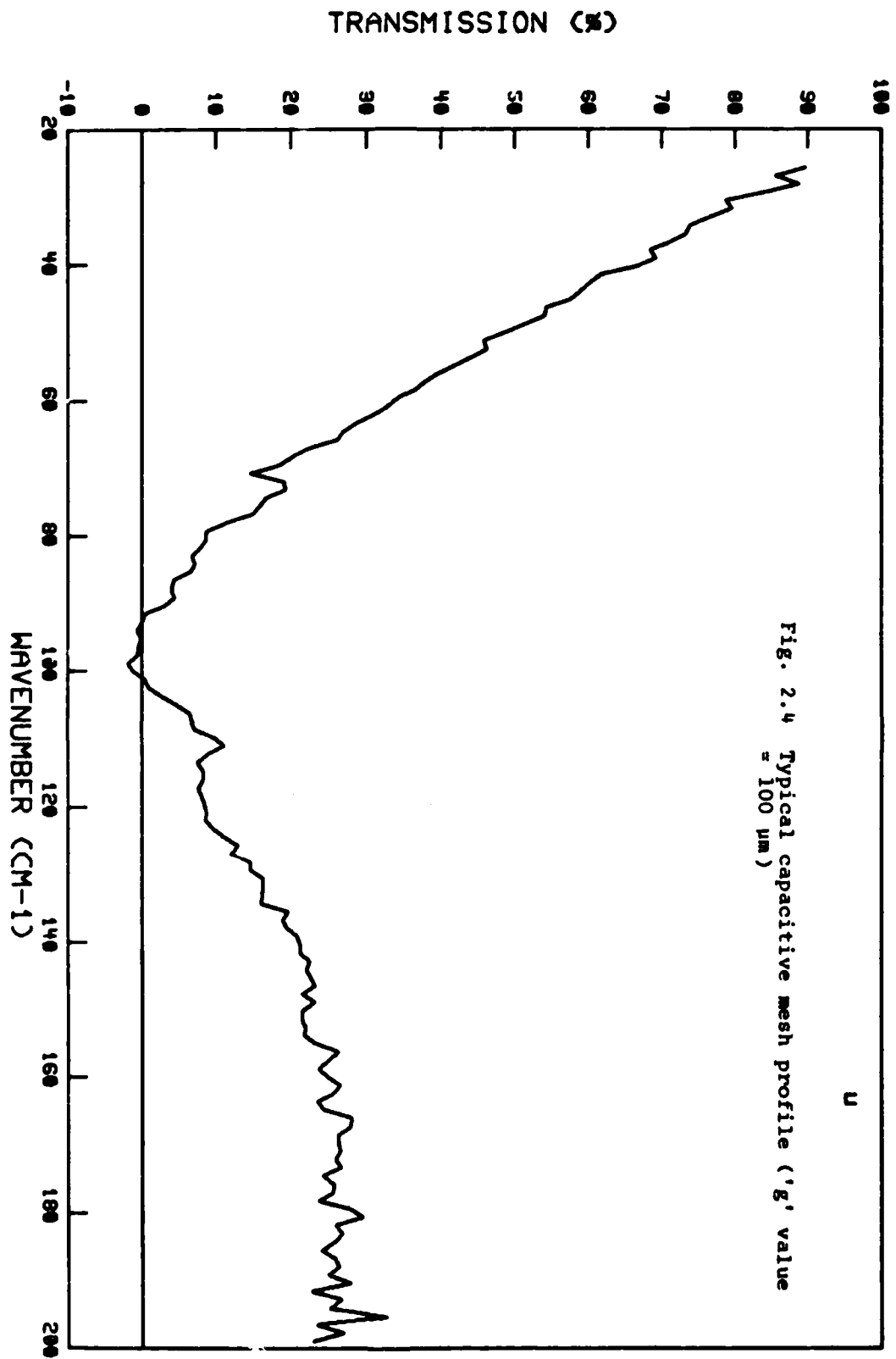


Fig. 2.1 Transmission profiles of inductive meshes, 100 L.P.I. to 500 L.P.I.







No. of lines per inch (L.P.I.)	Metal	Effective g value (μm)	z_{O}^{I}	a/g
100	copper	285	1.1	0.22
150	copper	200	0.9	0.26
250	copper	116	1.0	0.24
400	nickel	74	1.4	0.15
500	copper	59	1.0	0.24
750	copper	40	0.65	0.35
750	nickel	40	0.75	0.31
1000	copper	29	0.575	0.38
1000	nickel	29	0.8	0.29
1000	copper	29	0.96	0.25
1270	copper	25	0.54	0.39
1500	copper	21	0.50	0.40

Table 2.1 Details of the available inductive meshes

No. of lines per inch (L.P.I.)	Metal	Effective g value (μm)
30	Aluminium	25
46	"	32.6
70	"	51
141	"	54
282	"	103
605	"	202
686	"	400
1016	"	597
1411	"	919

Table 2.2 Details of available capacitive mesh